A PREVENTED SPARK REACTOR FOR POLLUTANT CONTROL. INVESTIGATION OF NO_X REMOVAL

Raïda Hafez, Sophie Samson, Emmanuel Marode

Laboratoire des Gaz et des Plasmas, Equipe Décharge Electrique et Environnement SUPELEC, Gif/yvette, France

Abstract: A non-thermal plasma reactor is investigated in view of NOx removal from exhaust gas of electrical plants. The plasma of the reactor is based on a prevented spark regime. A gas control system allows to introduce mixtures of gas composed of N_2, O_2, NO, H_2O. The densities of NO and NOx are measured using a chemiluminescent device. Results on NO removal introduced in the range of 20 to 700 ppmv are presented, with energy consumption per removed molecule. An attempt to model the chemical reactions due to the discharge is given.

Introduction NO_X removal is of an important concern in the attempt to control pollution due to exhaust flue gases from various sources ranging from power plants to car exhaust. There are many NO_X elimination technologies available, each having its own advantages and disadvantages [1]. Among these technologies, are conventional technologies such as Selective Catalytic Reduction (SCR). Techniques based on direct volume dissociation of molecular species by electron collisions have been investigated using various ways to produce the energetic electrons. The Electron-Beam techniques, which consist of spreading into the flue gas a beam of energetic electrons through a window, has been widely studied. All these technological approaches have already gained commercial acceptance. Another way to produce these electrons is through non-thermal electrical discharges, corona and silent discharges. The expected advantages are, first, that no external means for electron production is needed since the discharge develops in the gas bulk, and, secondly, the delivered energy may be mainly stored in the electron kinetic energy on a energetic level adapted to the dissociation process. Promising results have been already obtained by means of corona discharge irradiation. Industrial-scale experiments have been performed at the coal-burning power station of ENEL in Marghera near Venice in Italy [2,3,4].

We present here an extension of the non-thermal corona approach which consists of controlling the phase towards spark induced by positive streamer in point to plane gaps. That explains the label "prevented spark" given to such operating mode. It is not thermal, since the growth towards the spark is controlled in such a way that ETL will not be reached. Within the produced plasma the electron temperature T_e and

heavy species temperature T_g remain different and may both be varied. The physics of this regime has been discussed in [5]. A plasma reactor has been built consisting of some 26 discharges running on the basis of such prevented spark regime. The aim of this work is not to present a yet optimised reactor, but rather to investigate the properties of such device by showing its potentialities.

Experimental set-up The schematic layout of the experimental set-up is shown in fig. 1. A mixture of different bottled gases (N_2, O_2, NO, SO_2,NH_3) can be used to simulate the test flue gas. However no SO_2 and NH_3 introduction has yet been investigated. Each gas concentration is governed by an electronically controlled mass flowmeter, thus permitting the introduction of various gas combinations with a good precision. The flue gas to be processed is mixed and drawn to the reactor through a 50 cm stainless steel duct which can be heated so as to allow water admission in the form of water vapour. The heater provides variation of the gas temperature up to 80°C, thus allowing a variation of water vapour concentration up to 10%. Next, the flue gas passes through the reactor where it is energized by discharges produced within 26 couples of electrodes in point-plate configuration. Each discharge gap has its own electric circuit (Z,C_0, C, R) used to control the intensity of the needed prevented spark phase.

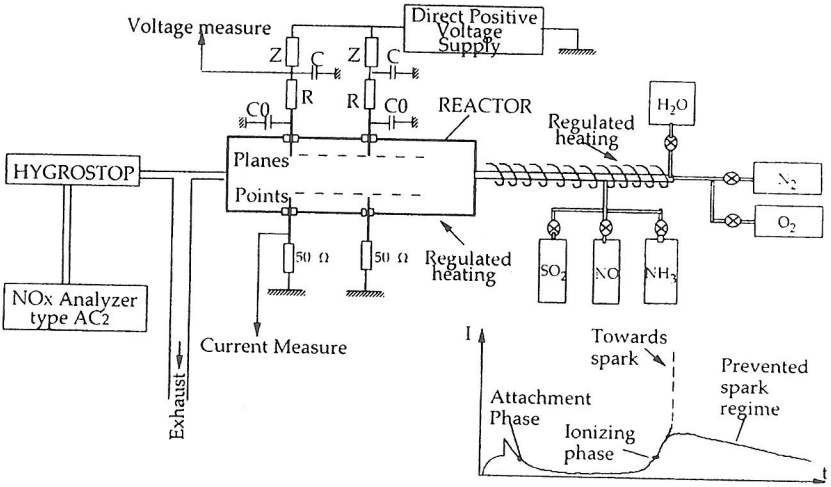

Fig. 1. Experimental set-up and schematic current evolution

The working regime is illustrated by the current sketch for each individual discharge cell, drawn in fig. 1. When the applied potential is large enough (some 8 kV for 0.6 cm gaps) succesive individual discharges appear, set here at 500 Hz. Shortly described, the initial rise is associated with the streamer propagation which establishes a filamentary plasma in which electrons disappear due to attachment into the electronegative gas component(labelled as the attachment phase). After gas expansion

[6], the field-to-neutral-density ratio E/N rises, and a new phase, labelled ionising phase, is set which normally leads to spark breakdown. When the applied high voltage is large enough, the current in each cell should evolve following the dotted line which corresponds to the spark formation. Instead, it follows the continuous line forming a non-thermal prevented spark plasma. Shortly explained, the capacity C_0 which actually is the stray capacity of the point electrode, contains enough energy to sustain the discharge until it reaches the ionising phase. After that, the discharge is sustained by the capacity C which delivers its energy through the resistance R which limits the delivered current. Roughly, the value of R is related to the heavy species temperature evolution, while the value of C will define the plasma life time.

In order to avoid water condensation inside the reactor, a heating wire was incorporated in the base of the cell. The main output of the reactor is opened to atmospheric pressure while a sample gas is extracted at the lateral side and fed to the diagnostic device, a chemi-luminescence analyser (AC2- Environnement S.A.). In order to avoid water condensation in the analyser, an appropriate apparatus (Hygrostop) was put upstream of the NO_X analyser to trap water vapour; the condensed water can eventually be collected for pH analysis. Temperature and humidity of the flue gas are measured with a probe placed upstream of the reactor.

Numerical modelling. Chemical reactions induced within the streamer filamentary discharge in air, at atmospheric pressure, are computed. Actually a full 2D time resolved model for the streamer development and its chemical activity is available and will be presented this year in Japan [7]. However this model deals only with the first discharge phase and does not include neither hydrodynamic phenomena nor the ionising spark formation phases is used here. Indeed the chemical kinetic is based on spectroscopic indications of the electron and neutral temperature evolution $T_e(t)$, $T_g(t)$ as well as the electron density $n_e(t)$ during the various discharge phases. The temporal evolution of N_e, T_e and T_g is sketched in fig. 2, where the various discharge phase, streamer, attachment and ionising phase may be identified. However, when the discharge stops an additional phase must be taken into account, which corresponds to the gas cooling phase. This phase strongly influences the chemical kinetics. The dynamic of the whole process involves time scales ranging from less than a nanoseconde (streamer phase) to more that one milliseconde (chemical cooling phase) so that a logarithmic time scale is needed. A set of coupled differential equations, including electron collision rates and heavy species reactions are solved with these discharge boundary conditions.

$$\frac{\partial \bar{y}(t)}{\partial t} = f(\bar{y}, t) \qquad \bar{y}(0) = \bar{y}_0$$

where the vector $\bar{y}(t)$ represents the various computed densities of O, N, NO, NO_2, N_2O, NO_3, N_2O_5, O_3, O_2,N_2, $N_2(v)$, (vibrational nitrogen) H_2O, OH.
156 different reactions are taken into account. Let us stress that the neutral temperature has two main effects. Well known is the temperature dependence of the Arhenius law of reaction between heavy species:

$$k = A T_g^{\,n} \exp(-\frac{C}{T_g})$$

which will strongly influence the reaction kinetics during the cooling phase. A, n and C are constants specific to each reactions.
Another effect is the fact that neutral density N decreases with increase of the gas temperature, so that the corresponding change of E/N strongly influence the electron temperature T_e and all the electron reaction rates.

Experimental results. The NO removal was studied in a simulated flue gas at atmospheric pressure and with a constant flue rate of 8 l/min. The electrical parameters (Z, C, R) were fixed to (68M, 15pF, 100K), the applied voltage to 9 KV and the gap distances to 4 mm. Mixtures of the kind of 98% of N_2, 2% of O_2, x% of H_2O and y ppm of NO, with variable x and y, are used to model the flue gases. Since the aim was to investigate the basic chemical mechanisms, the most simple situation has been first tested: a mixture, at room temperature, containing only pure N_2 and NO. Fig. 3. shows the amount Δ[NO] of removed NO concentration, in ppmv, as a function of the [NO] concentration initially introduced. A slight increase of the removal amount is observed with the increase of NO. Further, when O_2 is introduced, the removal efficiency is strongly reduced. Finally, if water is added to the mixture, heating all the device to 70° C in order to allow larger concentration of water vapour, the loss of efficiency due to the presence of O_2 is largely balanced, and reaches levels above that of pure N_2. Fig. 4, demonstrates that there is an optimum value in water concentration, with a maximum efficiency at some 5%. The energy cost per removed molecule passes through a minimum of 70 eV/mol. For that only the energy input into the discharge, i.e. the integral of the product of the gap potential per the discharge current V(t)*i(t), is taken into account, leaving the energy loss into the external resistance out from the estimation (a final device should use inductance instead of resistance). This figure may still be somewhat improved.
To be stressed is the fact that in all these measurements no significant other nitride oxides such as NO_2 or N_2O have been detected.

Modelling and discussion. From spectroscopic measurements, the temperature of the heavy species within the prevented spark may vary according to the value of R and C. From rotational temperature, an estimated temperature of 2500 K is adopted for computation. Since the gap potential during the prevented spark is 2KV, the corresponding E/N is about 150 10^{-17} V.cm^2. This value explains the 2.5 eV taken for the electron energy within the prevented spark. Four phases can be distinguished within the evolution dynamic, fig. 2: the streamer phase, the attachment phase, the ionising phase with the prevented spark, and the heavy species cooling phase during which no more current flows. There are obviously uncertainties in the values of reactions constants. The value of the dissociation rate k_{no} of NO by electrons is however the most difficult to estimate. The guess for k_{no} is taken between the dissociation rate of N_2 and O_2 by electron taking into account that the dissociation energies are 9.75, 6.48 and 5.08 for N_2, NO and O_2 respectively. For electron

energies of 16, 2.5 and 1,4 eV, k_{no} has been taken respectively as $2.5\ 10^{-9}$, $5\ 10^{-10}$ and $2.5\ 10^{-10}$.

If only a mixture of N_2 and NO is introduced, the modelling uses 64 reactions (among which only few affect really the numerical results). Fig. 5 shows what could happen. During the prevented spark phase, NO dissociates because of direct electron dissociation, and by the reaction

$$N+NO \rightarrow N_2 + O$$

Indeed, N is formed by N_2 dissociation by electron and also each time NO is dissociated. It follows that the NO removal within the discharge is quite complete and that atomic nitrogen and oxygen are left in the gas. During the cooling phase, the atomic O may only recombine into O_2 since no more NO is present for conversion into NO_2, this is in agreement with experimental observations. The atomic N may either recombine into N_2 or diffuse outside the discharge core, leading to further NO dissociation into the outer surrounding part. While the discharge radius should be in the range of 100 μm, an "effective" radius of NO removal should be considered. If a figure of 250 μm for the discharge radius is taken, the computed curves fit fairly well the experimental observations as seen on fig. 3.

If O_2 is added in the computation the removal efficiency drops strongly, in agreement with the experiment. The last case is the addition of H_2O which, as in the experimental case, balances the effect of O_2, while NO removal is due to the production of HNO_2 acid. This time however the computation results do not fit at all the experimental observations more efficient. A basic explanation should be that in such high amount of water vapour, clustering of water droplets could play a dominant role as suggested by the work at Kurchatov Institute in Moscow [8]. Droplets may incorporate NO molecules and acidify them inside the droplet.

Conclusion. The prevented spark phase seems to demonstrate some efficiency in promoting the formation of radicals from gas dissociation and fostering pollutant conversion into other species less harmful or easily taken away. It should be stressed that no addition of external catalytiq product such as NH_3 has been used in this experimental approach. The measurement of the water acidity was clearly positive, and a complete experimental check of the overall conservation law of the various substances is under investigation.

[1]"Non-Thermal Plasma Techniques for Pollution Control-NATO ASI Series, Penetrante M. & Shultheis E., ed, vol 34 (1993)
[2]S.Masuda, *Pure & Appl. Chem.* Vol.**60**, No-5, pp.727-731 (1988)
[3]G.Dinelli, L.Civitano,M.Rea, M.,*IEEE Trans. Ind. Appl.* **25**, 535-541.(1990)
[4] I.Gallimberti, Pure & Appl.Chem, 60,5,663-674(1988)
[5]E.Marode, A.Goldman, M.Goldman, NATO ASI Series, vol 34, A,167-190(1993)
[6] E.Marode,NATO Series ASI ,Series B, Volume 89b,119-166 (1981)
[7] D.Djermoune et al, 11th Gas Disch. and their Appl., Tokyo, Sept (1995).
[8] B.V.Potapkin et al, NATO ASI Series, vol 34, A,91-106(1993)

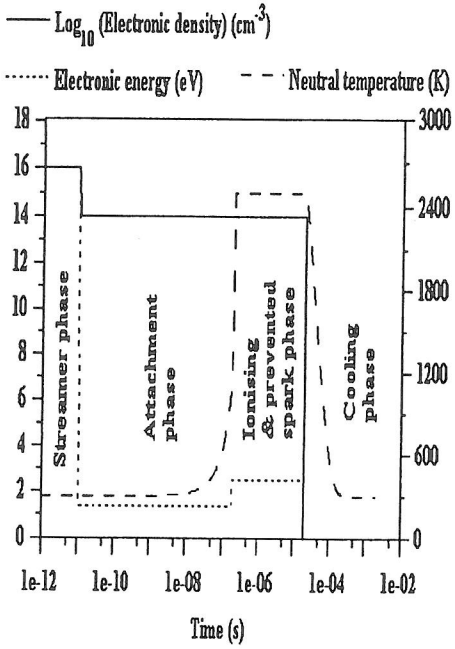

Fig. 2. Initial conditions

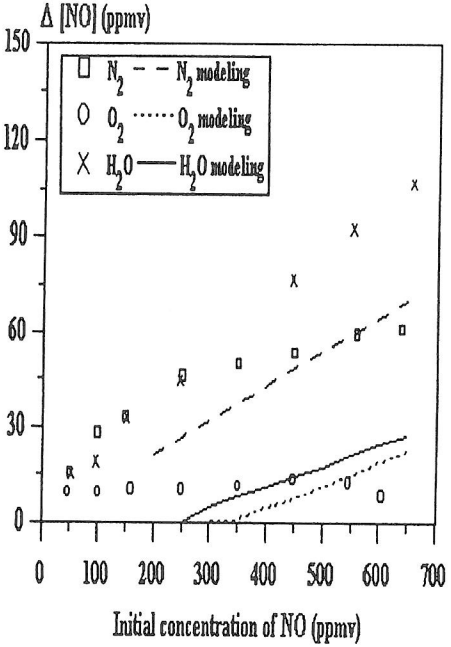

Fig. 3. Experimental and numerical results

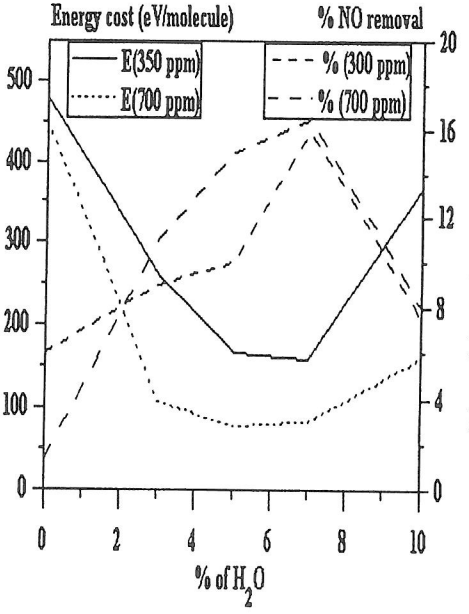

Fig. 4. Optimum in removal with water

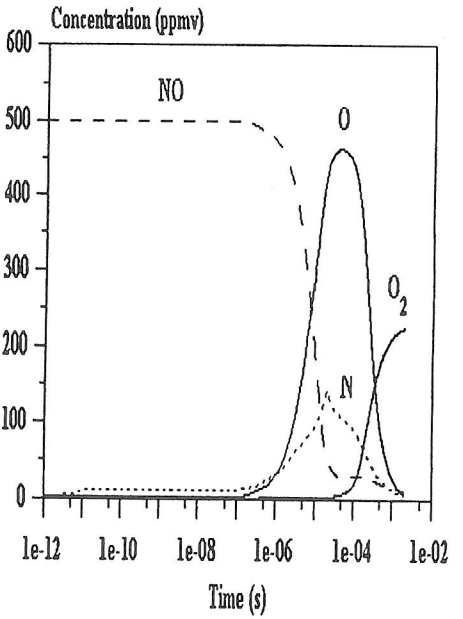

Fig. 5.Species density evolution